Journal of Magnetism and Magnetic Materials 324 (2012) 140–145

Contents lists available at ScienceDirect

Journal of Magnetism and Magnetic Materials

journal homepage: www.elsevier.com/locate/jmmm

Synthesis and characterizations of microwave sintered ferrite powders and their composite films for practical applications

S.R. Shannigrahi *, K.P. Pramoda, F.A.A. Nugroho

*Institute of Materials Research and Engineering, A*STAR (Agency for Science, Technology and Research), 3 Research Link, Singapore 117602, Singapore*

ARTICLE INFO

Article history:
Received 18 May 2011
Accepted 26 July 2011
Available online 7 August 2011

Keywords:
Ferrite
Microwave sintering
EMI shielding

ABSTRACT

Phase pure single phase ferrite powders of $(Ni_xR_{1-x})_{0.5}Zn_{0.5}Fe_2O_4$ (R=Mn, Co, Cu; x=0, 0.5) were manufactured using microwave sintering at 930 °C for 10 min in air atmosphere. The powders were characterized for their structure, microstructure, thermal, and magnetic properties. Selected powders were used as fillers to prepare their composite films using polymethyl methacrylate polymers as matrix. The composite films were prepared using the melt blending approach and were tested for their microstructure, thermal, and magnetic hysteresis loop as well as 3D magnetic field space mappings using an electromagnetic compatibility scanner. Among the studied ferrites, cobalt doped ferrites and their composites showed the best electromagnetic interference (EMI) shielding effectiveness value and have potential for practical EMI shielding applications.

1. Introduction

Ferrites are technologically very important materials because of their high magnetic permeability, low core loss, and soft magnetic nature, which make them suitable for different applications like electrical components, memory devices, and magnetostrictive devices as well as electronic components such as transformers, choke coils, noise filters, recording heads, etc [1–7]. Thus ferrites have been extensively studied by several researchers with different endeavors [5–9]. A number of researchers have endeavored to prepare ferrite materials in different forms [10–12]. Ferrites prepared by the conventional ceramic method involve high temperature, which can result in the loss of their fine particle size. The bulk properties of the similar type of ferrites differ among compositions. In the recent years many works have been focused to establish possible cost effective manufacturing–processing scheme to optimize technologically important parameters [13–18]. Verma et al. have reported the development of a new ferrite with low power loss based on manganese nickel zinc ferrite composition for switch mode power supplies [19]. Several other works have been reported on sintering behavior, including densification and grain growth of NiCuZn ferrites and their modified forms using microwave (MW) heat treatment [20–28]. Bhaskar et al. have reported low power loss MgCuZn ferrites using the MW sintering method [29]. Yadoji et al. have reported the comparative property studies of $Ni_{1-x}Zn_xFe_2O_4$ prepared using conventional and MW techniques with the set sintering recipe of 1275 °C for 30 min [30]. It is reported that the properties of base $NiZnFe_2O_4$ can be further improved by introducing suitable modifiers like Mn, Cu, Co, Cu etc. So, the search for new modified ferrites as well as the cost effective processing recepies is very much active in current ferrite materials research. To the best of our knowledge, no report has been published on a systematic investigation of MW sintering of $(Ni_xR_{1-x})_{0.5}Zn_{0.5}Fe_2O_4$ (NRZF); (R=Mn, Co, Cu; x=0, 0.5). In view of the importance of these materials and the utilization of MW sintering, in this work we have prepared NRZF ferrites through a one stage sintering process using MW and prepared their composite films, and studied their structure, microstructure, thermal, and magnetic properties.

2. Experimental procedure

2.1. Ferrite powder synthesis

The ferrite powders of $(Ni_xR_{1-x})_{0.5}Zn_{0.5}Fe_2O_4$ (NRZF) [R=Mn, Co, Cu; x=0, 0.5] were prepared by a one stage heat treatment process using a multi-mode MW tube furnace with the magnetron frequency of 2.45 GHz (MW-T0316V, Syno-Therm) the maximum operating temperature up to 1400 °C, and 0.5–3 kW (Fig. 1a). An adjustable electrical control system was used to control the energy to be delivered to the sample at a programmed rate. The heating chamber was a double walled, stainless steel, water cooled tubular cavity that stayed cool to touch, even when processing temperature was ~ 1400 °C. Inside the chamber was a high purity quartz crystal cylinder where samples were loaded for processing. The temperature was recorded using a high precision optical pyrometer. Stoichiometry mixtures of the individual

* Corresponding author. Tel.: +6568748299; fax: +6568720785.
E-mail address: santi-s@imre.a-star.edu.sg (S.R. Shannigrahi).

0304-8853/$ - see front matter © 2011 Elsevier B.V. All rights reserved.
doi:10.1016/j.jmmm.2011.07.050

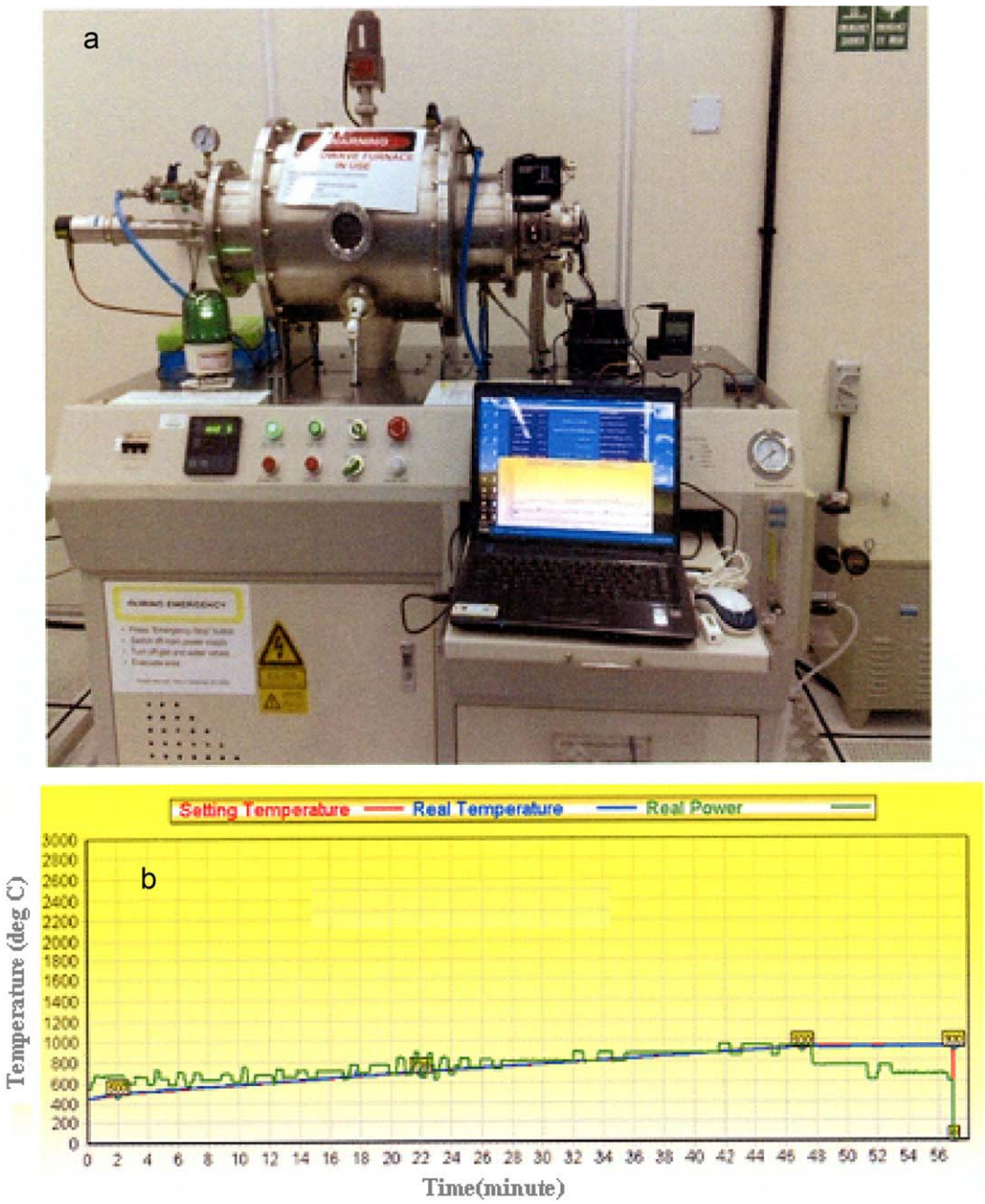

Fig. 1. (a) Microwave furnace and (b) the annealing recipe.

oxides (99.995%, Sigma-Aldrich) were wet milled with powder and ball ratio of 1:5. The mixtures were further dried by keeping them inside an oven at 100 °C for overnight. Dried mixtures were consolidated into disk form by a uniaxial hydraulic press at room temperature and sintered using MW by keeping them inside a Quartz crucible. During the MW sintering of the samples, temperature was measured using an infrared pyrometer. The crucible was surrounded by SiC plates, which act as susceptors to provide initial heating of the compact disk samples. Once the materials are sufficiently hot they will couple/absorb MW effectively and will get heated directly, including the core. The secondary purpose of SiC is to maintain the surface temperature. The crucible was positioned at the center of the furnace, where the MW radiation is the strongest. The disks were heated in atmospheric air ambient at temperatures ranging from 900 to 950 °C for 10 min at a heating rate of 20 °C/min by varying the magnetron power between 1000 and 2500 W followed by normal furnace cooling. The MW annealing recipe as shown in Fig. 1(b) was employed. The details of the heating mechanism were discussed elsewhere [23,30].

2.2. Polymer composite preparation

To prepare the composite films the MW processed ferrites disks were ground and sieved using a 325 mesh (<45 μm). These powders were used as fillers with varying loading amount of 20–70wt% in a thermoplastic matrix of polymer like polymethyl methacrylate (PMMA). The films were prepared using the melt blending approach. A dry mixture of ferrite powders and polymers were placed inside the melt extruder to prepare rod shape composites, which were further hot pressed to produce composite films. The overall thicknesses of the composite films were kept below 1 mm.

2.3. Characterization of ferrite powders and their composite films

Phase analysis and microstructures of powders and composite films.

The phase formation and crystalline quality of the MW sintered individual ferrite powders were studied by x-ray diffraction (XRD) with a powder diffractometer, Bruker General Area Detector Diffraction System (GADDS), in a wide range of Bragg angle ($20^\circ < 2\theta < 60^\circ$) at room temperature using Cu K_α radiation ($\lambda = 0.15418$ nm). The microstructures of the ferrites as well as their composite films were examined by scanning electron microscopy (FESEM, JSM-6700F, JEOL Ltd) and transmission electron microscopy (HRTEM, JEOL 2100). Identical magnifications were taken for every measurement. Particle sizes of the ferrites and the polymer composites were determined from the SEM and TEM micrographs.

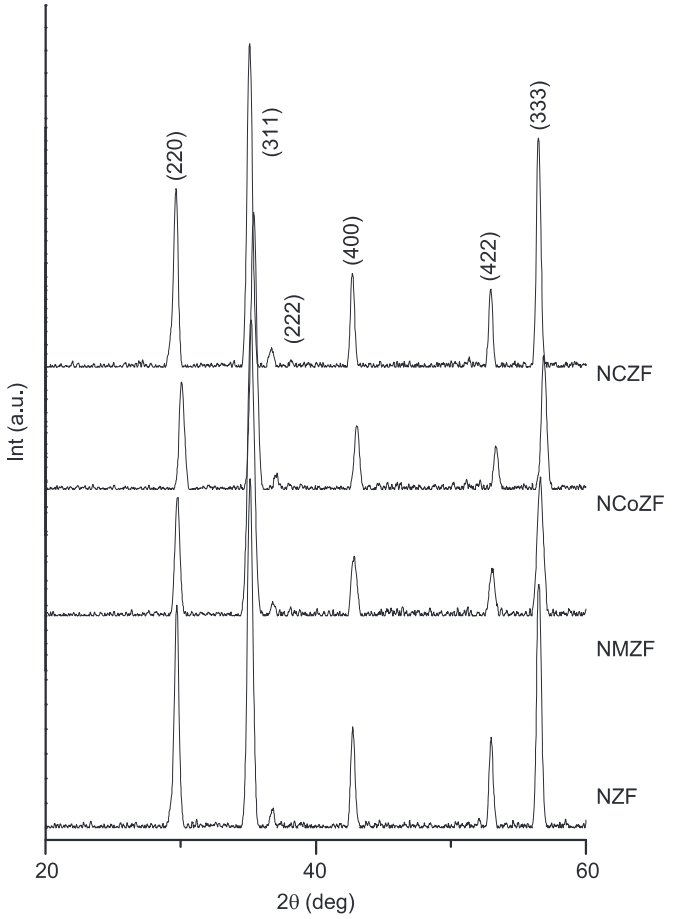

Fig. 2. Room temperature XRD spectra of the $(Ni_xR_{1-x})_{0.5}Zn_{0.5}Fe_2O_4$ (NRZF) (R=Mn, Co, Cu; x=0, 0.5) ferrite powders prepared using microwave techniques.

2.4. Thermal properties

Thermal stability of the polymers and the composite materials was studied using a thermogravimetric analyzer (TGA, TA instruments Q500, USA). The measurements were carried out from room temperature to 800 °C at a heating rate of 10 °C/min in air atmosphere.

2.5. Magnetic hysteresis parameters and 3D magnetic field mapping

A vibrating sample magnetometer (VSM, Lakeshore Cryotronics Inc., USA) was used to evaluate the room temperature magnetic hysteresis parameters of the fillers and the polymer composites. The samples were weighed and covered with aluminium foil to mount the sample on the sample holder with the help of a Teflon tape. 3D magnetic field mapping as well as the electromagnetic interference (EMI) shielding effectiveness values of the composite films were measured using an electromagnetic compatibility (EMC) scanner (Langer EMV-Technik chip scan V1.214).

3. Results and discussion

3.1. Structure–morphology

Room temperature XRD patterns of the MW sintered powders are shown in Fig. 2. The sharp and single diffraction peaks indicate good homogeneity and crystallization of the samples. There is no change in the basic spinel cubic structure. However, a slight shift in the peak positions and some changes in the intensity of a few reflections have been observed for the samples doped with different dopants. This may be due to the variation of crystallite sizes caused from doping of the different dopants with different ionic radii like 0.46, 0.745, 0.69 and 0.73 Å, respectively, for Mn, Co, Ni, and Cu ions. The individual lattice parameters are calculated using standard software and refined (using least-square method) using a computer package (PowdMult) and the values are found to be 8.104, 8.4139, 8.4493, and 8.4658 Å respectively [31]. The substitution of Mn ions in place of Ni ions results in decrease of lattice parameters, because of the smaller size of the substituted ions, whereas lattice parameters increase on substituting Cu ions in place of the Ni ions, owing to their smaller size. Scanning electron micrographs (SEM) of cobalt doped NZF powder are shown in Fig. 3(a). The micrographs reveal

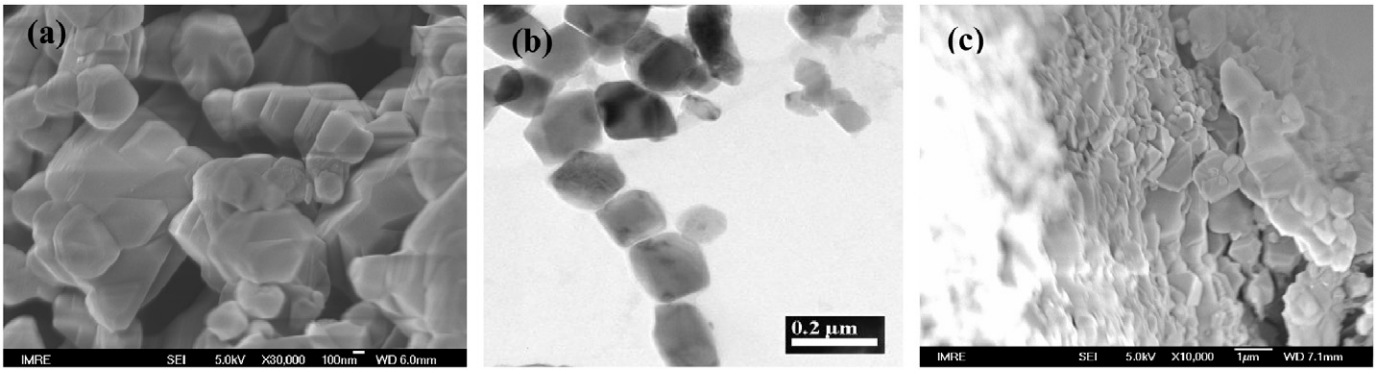

Fig. 3. Ferrite powders as observed by (a) SEM and (b) TEM and (c) surface morphology of the composite films as observed by SEM.

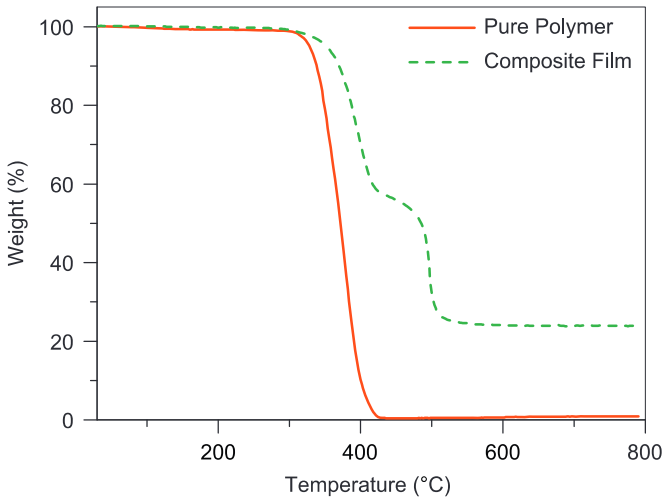

Fig. 4. Thermal stability study using TGA analysis.

big and uniform particle size of the powder samples. Micron size hexagonal morphologies are observed, which are also confirmed through TEM analysis (Fig. 3(b)). The morphology of the composites depicts that the ferrite particles are embedded uniformly in the polymer matrices as shown in Fig. 3(c).

3.2. Thermal behavior

Fig. 4 shows a representative TGA thermogram of the composite film with NCoZF ferrites as the filler and PMMA as the base matrix. The graphical data was analyzed using TA instruments (universal analysis advantage software). The composite films are found to be stable at a higher temperature of more than 30 °C compared to the host polymer matrix. This improvement can enhance the applications of the composite films in certain harsh environments. The overall composite films were thermally stable up to 300 °C.

3.3. Magnetic behavior

Fig. 5(a) and (b) depicts the room temperature magnetization versus magnetic hysteresis (M–H) loops for the MW sintered ferrite powders as well as their composite films with PMMA polymer matrix. All the powder samples are magnetically quite soft in nature and among them, cobalt doped ferrites have the highest magnetization values. The magnetization value diminishes once the ferrites form composites. This is likely the screening effect by the non-magnetic component like PMMA matrix [4]. Fig. 6(a) depicts the 3D magnetic field space mapping of the composite film formed using a combination of NCoZF and PMMA. The applied input power using a strip line was −20 dB m, and the frequency range of 5–50 MHz. The field distribution across the films apparently seems similar, which indicates the homogeneous distribution of ferrite fillers in the PMMA matrix. Fig. 6(b) depicts the EMI shielding effectiveness values measured for the NCoZF and PMMA composite films at room temperature in the frequency range of 500 kHz– 120 MHz using the EMC scanner. The shielding effectiveness trend as shown in Fig. 6(b) supports the homogeneous magnetic properties of the composite films and the composites can be useful for practical applications as EMI shielding materials.

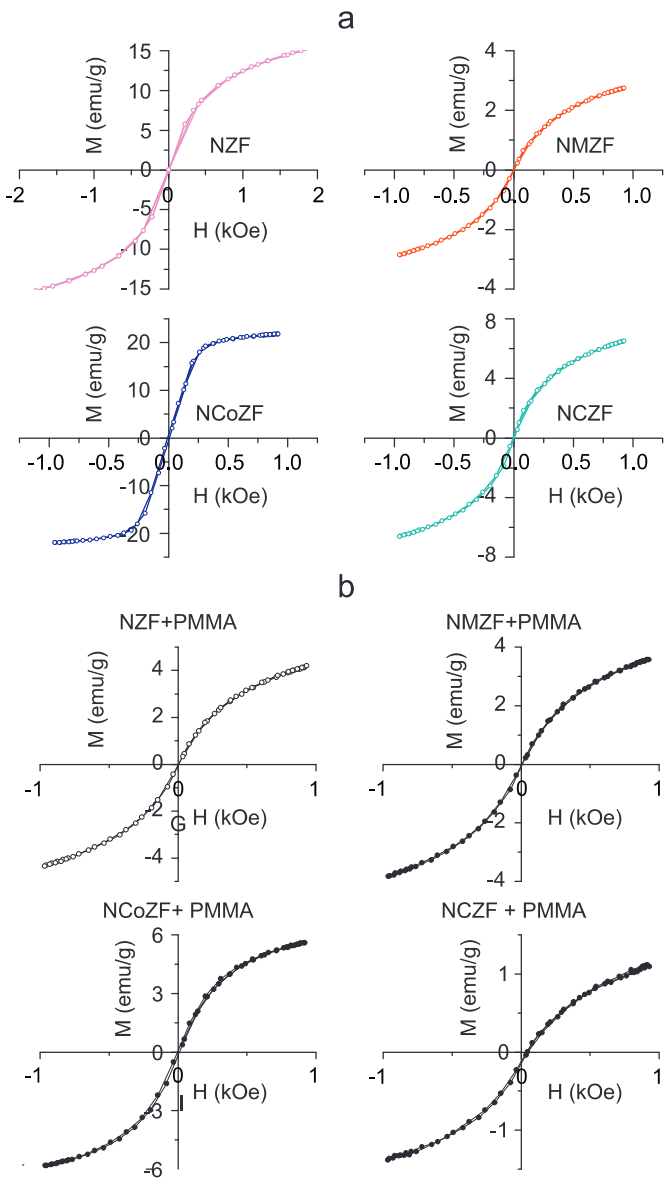

Fig. 5. Room temperature M–H loops of the (a) ferrite powders and (b) their composites using PMMA polymers.

4. Conclusions

Ferrite powders of $(Ni_xR_{1-x})_{0.5}Zn_{0.5}Fe_2O_4$ (NRZF) [R=Mn, Co, Cu; x=0, 0.5] were prepared by a one stage heat treatment process at 930 °C for 10 min in atmospheric air using a MW furnace. Phase pure single phase with micron size hexagonal morphologies were observed for the ferrite powders as analyzed by XRD. Morphologies of the ferrites as well as their composites depict that the ferrite particles were embedded uniformly in the polymer matrices. TGA analysis showed that thermal stability of the composites found improved by 30 °C compared to the host matrix. Both the ferrite powder and their composites exhibited a soft magnetic nature as observed from hysteresis loop. The 3D magnetic field mapping of the composite cobalt doped NZF reveals the homogeneous distribution of ferrite particles in the polymer matrix. The EMI shielding tests also support the homogeneous magnetic properties in the composites and their potential applications as EMI shielding materials.

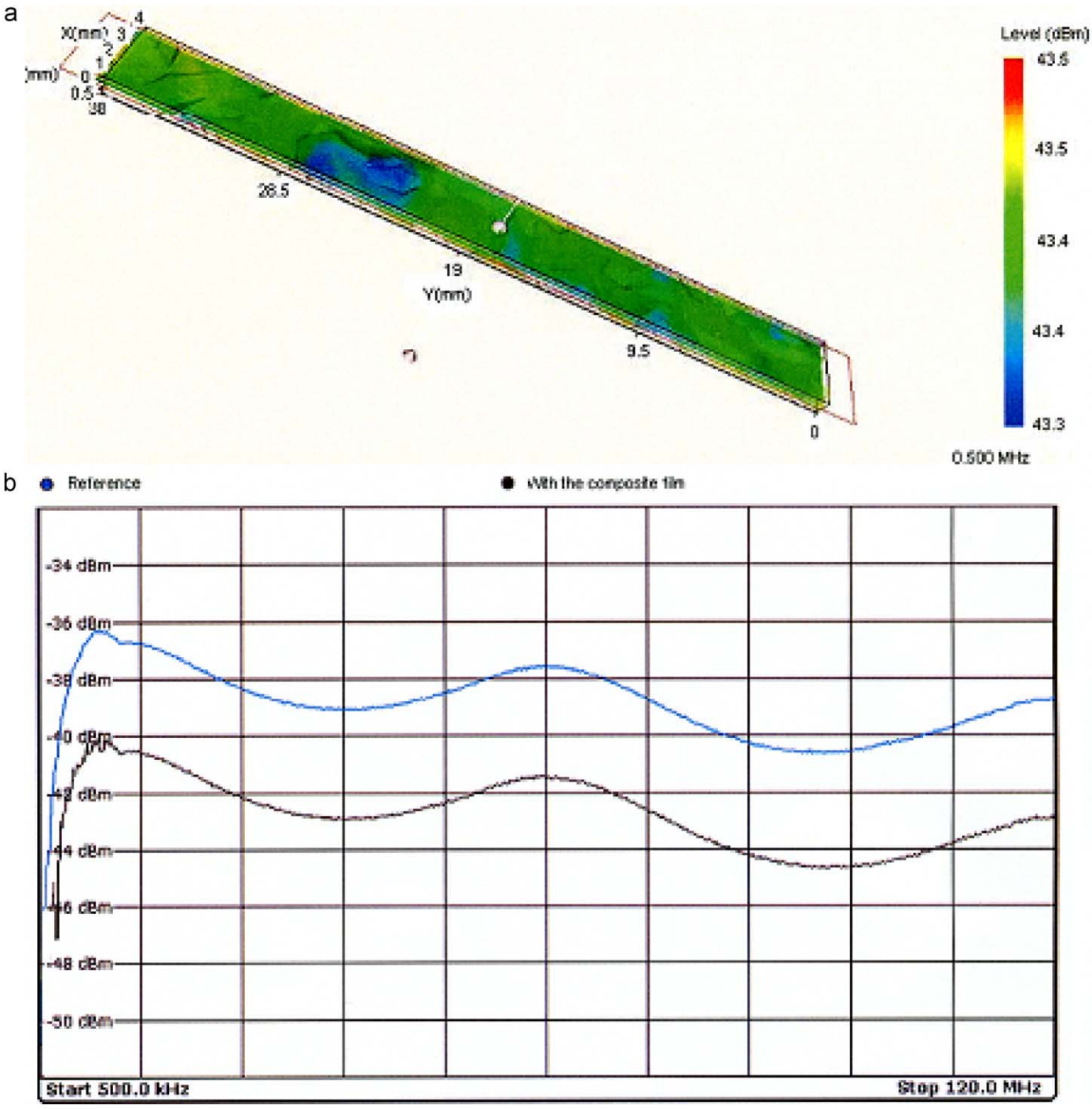

Fig. 6. (a) 3D magnetic field space mapping of the composite film using the input power of −20 dB m, at a frequency of 5–50 MHz of the composite films prepared using a combination of NCoZF and PMMA and (b) EMI shielding effectiveness value measured at room temperature in the frequency range of 500 kHz – 120 MHz.

References

[1] T. Tada, US Patent 20090057606A1, 2008.
[2] J. Sláma, R. Dosoudil, R. Vícen, A. Grusková, V. Olah, I. Hudec, E. Ušák, J. Magn. Magn. Mater 195 (2003) 254–255.
[3] V.R.K. Murthy, J. Sobhanadri, B Viswanathan, Rev. Roum. Phys 22 (1977) 821.
[4] K.S. Moon, C.P. Wong, S.H. Kim, H.D. Choi, S. Han, H.G. Yoon, K.S. Suh, J. Electron. Mater 36 (2007) 1711.
[5] M.P. Reddy, G. Balakrishnaiah, W. Madhuri, M.V. Ramana, N.R. Reddy, K.V.S. Kumar, V.R.K. Murthy, R.R. Reddy, J. Phys. Chem. Solids 71 (2010) 1373.
[6] B. Li, Z.X. Yue, X.W. Qi, J. Zhou, Z.L. Gui, L.T. Li, Mater. Sci. Eng. B 99 (2003) 252.
[7] M.P. Reddy, P. Reddy, W. Madhuri, N.R. Reddy, K.V.S. Kumar, V.R.K. Murthy, R.R. Reddy, Physica Scripta 81 (2010) 055801.
[8] W.C. Hsu, S.C. Chen, P.C. Kuo, C.T. Lie, W.S. Tsai., Mater. Sci., Eng. B Solid 111 (2004) 142.
[9] T. Nakamura, J. Magn. Magn. Mater. 168 (1997) 285.
[10] H. Zhang, Z. Ma, J. Zhou, Z. Yue, L. Li, Z. Gui, J. Magn. Magn. Mater. 213 (2000) 304.
[11] C. Ventakataraju, Appl. Phys. Res. 1 (2009) 41.
[12] H. Saita, Y. Fang, A. Nakano, D. Agrawal, M.T. Lanagan, T.R. Shrout, et al., Jpn. J. Appl. Phys. 41 (2002) 86.
[13] R. Lebourgeois, S. Duguey, J.P. Ganne, J.M. Heintz, J. Magn. Magn. Mater 312 (2007) 328.
[14] J. Murbe, J. Topfer, J. Electroceram. 15 (2005) 215.
[15] M. Yan, J. Hu, J. Magn. Magn. Mater 305 (2006) 171.
[16] M. Kubli, L. Luo, I. Bilecka, M. Niederberger, Chimia 64 (2010) 170.
[17] J.J. Shrotri, S.D. Kulkarni, C.E. Deshpande, A. Mitra, S.R. Sainkar, P.S.A. Kumar, S.K. Date, Mater. Chem. Phys. 59 (1999) 1.
[18] A. Verma, A.K. Saxena, D.C. Dube, J. Magn. Magn. Mater 263 (2003) 228.

[19] Z. Yue, J. Zhou, L. Li, H. Zhang, Z. Gui, J. Magn. Magn. Mater 208 (2000) 55.
[20] T. Tsutaoka, J. Appl. Phys. 93 (2003) 2789.
[21] A. Verma, M.I. Alam, R. Chatterjee, T.C. Goel, R.G. Mendiratta, J. Magn. Magn. Mater. 300 (2006) 500.
[22] O.F. Caltun, L. Spinu, A. Stancu, L.D Thung, W. Zhou, J. Magn. Magn. Mater 242–245 (2002) 160.
[23] W. Madhuri, M.P. Reddy, N.R. Reddy, K.V.S. Kumar, V.R.K. Murthy, J. Phys. D: Appl. Phys. 42 (2009) 165007.
[24] Y.J. Yang, C.I. Sheu, S.Y. Cheng, H.Y. Chang, J. Magn. Magn. Mater. 284 (2004) 220.
[25] H. Su, H. Zhang, X. Tang, X. Xiang, J. Magn. Magn. Mater. 283 (2004) 157.
[26] C.Y. Tsay, K.S. Liu, T.F. Lin, I.N. Lin, J. Magn. Magn. Mater. 209 (2000) 189.
[27] A.S. Vanetsev, V.K. Ivanov, N.N. Oleynikov, Y.D. Tretyakov, Mendeleev Commun. 14 (2004) 145.
[28] C.W. Kim, J.G. Koh, J. Magn. Magn. Mater. 257 (2003) 355.
[29] A. Bhaskar, B.R. Kanth, S.R. Murthy, J. Mater. Sci. 39 (2004) 3787.
[30] P. Yadoji, R. Peelamedu, D. Agrawal, R. Roy, Mater. Sci. Eng. B 98 (2003) 269.
[31] E. Wu, POWD, An interactive powder diffraction data interpretation and indexing program, ver. 2.1, School of Physical Science, Flinders University of South Australia Bedford Park, S.A. 5042, Australia.